Received: 13 January 2021 | Revised: 10 February 2021 | Accepted: 21 February 2021

DOI: 10.1111/cbdd.13833

RESEARCH ARTICLE

WILEY

Design, synthesis, and biological evaluation of novel 4,4-difluoro-1-methyl-*N*, 6-diphenyl-5, 6-dihydro-4*H*-pyrimido [4, 5-*b*] [1, 2, 4] triazolo [4, 3-*d*] [1, 4] diazepin-8-amine derivatives as potential BRD4 inhibitors

Jiuhui Li[1] | **Wenjie Zhang**[1,2] | **Qianqian Qiu**[1] | **Daoguang Zhou**[1] | **Ziying Feng**[1] | **Zhenzhen Tong**[1] | **Jiaxin Wei**[1] | **Wenlong Huang**[1,2] | **Jieming Li**[3] | **Hai Qian**[1,2] | **Wei Shi**[1]

[1]Center of Drug Discovery, State Key Laboratory of Natural Medicines, China Pharmaceutical University, Nanjing, China

[2]Jiangsu Key Laboratory of Drug Discovery for Metabolic Disease, China Pharmaceutical University, Nanjing, China

[3]Henan University of Chinese Medicine, Zhengzhou, China

Correspondence
Jieming Li, Henan University of Chinese Medicine, Zhengzhou, China.
Email: jiemingli@hactcm.edu.cn

Hai Qian and Wei Shi, Center of Drug Discovery, State Key Laboratory of Natural Medicines, China Pharmaceutical University, Nanjing, China.
Emails: qianhai24@163.com; 1520200004@cpu.edu.cn

Funding information
National Science Foundation of China; China Postdoctoral Science Foundation

Abstract

Bromodomain-containing protein 4 (BRD4) plays an extremely important physiological role in cancer, and the BRD4 inhibitors can effectively inhibit the proliferation of tumor cells. By taking BI-2536 (PLK1 and BRD4 inhibitor) as the lead compound, sixteen novel BRD4 inhibitors with the 4,4-difluoro-1-methyl-*N*,6-diphenyl-5,6-dihydro-4*H*-pyrimido[4,5-*b*] [1,2,4] triazolo[4,3-*d*] [1,4] diazepine-8-amine structure were designed and synthetized. Among the target compounds, compound **15h** exhibited outstanding inhibition for BRD4-BD1 (IC_{50} value of 0.42 μM) in the BRD4-BD1 inhibitory activity assay. Additionally, cell growth inhibition assay demonstrated that compound **15h** potently suppressed the proliferation of MV4-11 cells (IC_{50} value of 0.51 μM). Besides, compound **15h** induced apoptosis and G0/G1 cycle arrest in MV4-11 leukemia cells effectively, and downregulated the expression of c-Myc in a dose-dependent manner. In summary, the optimal compound **15h** is expected to become the clinical therapeutic drug for further research.

KEYWORDS

anti-proliferation, anti-tumor, BRD4 inhibitors, cell apoptosis, c-Myc

1 | INTRODUCTION

Bromodomain-containing protein 4 (BRD4), a member of the best studied bromodomain and extra-terminal domain (BET) protein family and containing two tandem bromodomains (BD1 and BD2), regulates gene expression by recruiting transcription factors at specific gene transcription sites and binding to acetyl lysine (KAc) histones (Fu et al., 2015; Kharenko et al., 2018). The abnormal expression of BRD4 will activate the downstream gene c-Myc, which could increase the occurrence of cancers (Yoshida, 2018). Thus, disturbing the interaction between BRD4 and KAc protein can effectively inhibit the proliferation of tumor cells and the production of inflammatory factors (Chen et al., 2019; Ran et al., 2015; Wang et al., 2019; Zhou et al., 2019). Due to the extremely important physiological role, BRD4 has become an important target in anti-cancer field (Duan et al., 2018; White et al., 2019).

In recent years, several small molecules targeting BRD4 protein have been developed for cancer therapy, such as (+)-JQ-1 (**1**, Figure 1), I-BET-762 (**2**, Figure 1), OTX015

Jiuhui Li and Wenjie Zhang made equal contribution to this work.

(**3**, Figure 1), and BI-2536 (**4**, Figure 1; Andrikopoulou et al., 2020; Ciceri et al., 2014; Huang et al., 2016; Stathis et al., 2016; Zhao et al., 2013). Wherein, (+)-JQ-1 was the first reported BRD4 inhibitor, and has been employed widely to evaluate its therapeutic potential in a great many cancers (Filippakopoulos et al., 2010). I-BET-762, obtained from optimization of a hit which was designed to enhance ApoA1 expression and had entered clinical trials for NUT (nuclear protein in testis) midline carcinoma and other cancers (Delmore et al., 2011; Leal et al., 2017). OTX015 showed clinically effective activity with nontoxic doses in Phase I trials for NUT midline carcinoma and hematologic malignancies (Jung et al., 2015; Zhang et al., 2016). BI-2536 was a dual potent inhibitor of BRD4 and PLK1, which might provide a new strategy to treat acute myeloid leukemia (Liu et al., 2017; Steegmaier et al., 2007). Significantly, by exploring the docking assay of (+)-JQ-1 (Figure 2a), I-BET-762 (Figure 2b), and BI-2536 (Figure 2c) with BRD4-BD1, it was indicated that methyl triazole ring (red, Figure 1) and methylpiperazine-one ring (blue, Figure 1) could form hydrogen bonds with the residues Tyr97 and Asn140 which were the essential binding sites for the BRD4 inhibitors (Figure 2).

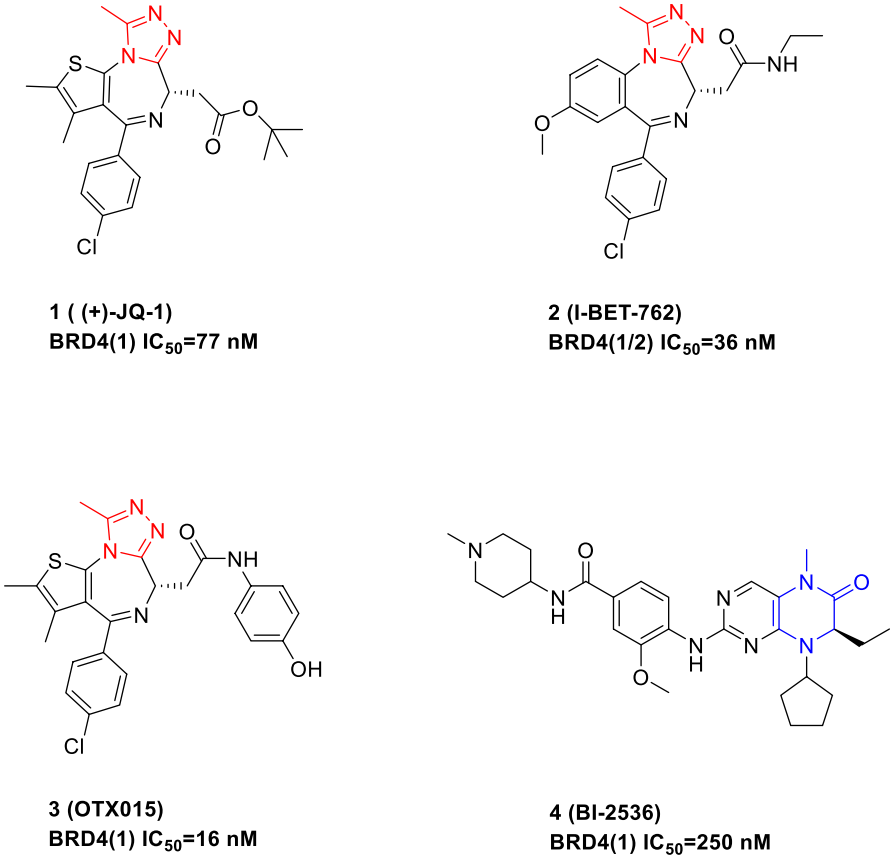

FIGURE 1 Structures of representative BRD4 inhibitors [Colour figure can be viewed at wileyonlinelibrary.com]

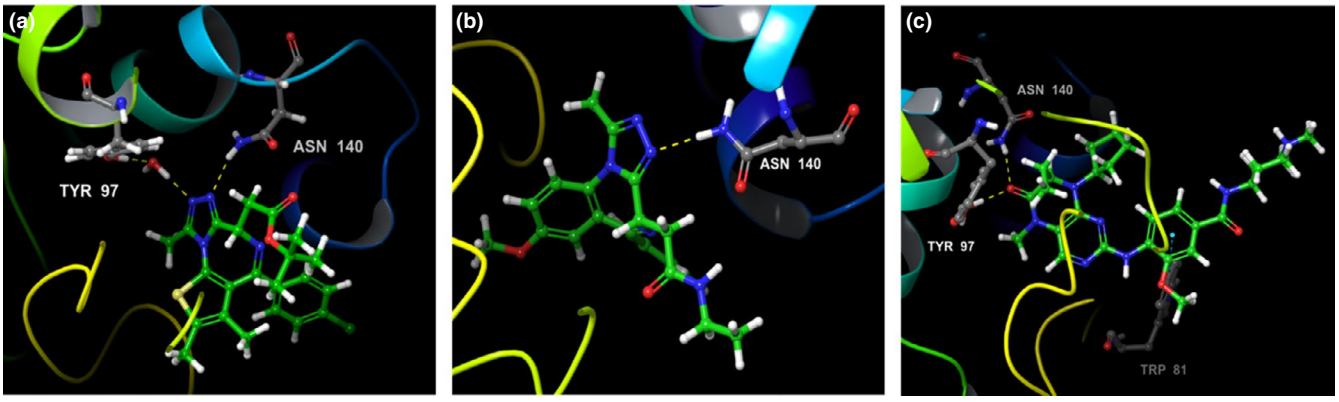

FIGURE 2 (+)-JQ-1, I-BET-762, and BI-2536 can form hydrogen bonds with the residue Asn140 of KAc recognition region in BRD4: (a) Eutectic structure of (+)-JQ-1 and BRD4 complex (PDB ID: **3MXF**); (b) Eutectic structure of I-BET-762 and BRD4 complex (PDB ID: **3P5O**); (c) Eutectic structure of BI-2536 and BRD4 complex (PDB ID: **4O74**) [Colour figure can be viewed at wileyonlinelibrary.com]

In this study, to develop the target compounds with high specificity for BRD4 inhibition, we focused on BI-2536 by performing extensive structure-activity relationships (SARs) study. According to the protein-ligand interactions, it was found that (*R*)-4-cyclopentyl-3-ethyl-1-methylpiperazine-2-one group (group I) could form essential hydrogen bonds with the residues Tyr97 and Asn140 in BRD4 (PDB ID: **4O74**; Chen et al., 2015). Furthermore, the more potent compounds could be obtained when group I of BI-2536 (IC_{50} value of 250 nM) was substituted with 1-cyclopentyl-6,6-difluoro-4-methyl-1,4-diazepan-5-one group (group II) of TAK-960 (IC_{50} value of 50 nM). In addition, it has been reported that 3-methyl-7-phenyl-9*H*-[1,2,4] triazolo[4,3-*a*] [1,4] diazepine group (group III) of OTX015 (IC_{50} value of 16 nM) could form essential hydrogen bonds with the residues Tyr 97 and Asn140 in BRD4, which was important to the inhibition for BRD4. Therefore, methyl triazole ring could be further combined with group II of TAK-960 to improve the specificity for BRD4 inhibition. Above all, we replaced group I with 9,9-difluoro-3-methyl-7-phenyl-8,9-dihydro-7*H*-[1,2,4] triazolo[4,3-*d*] [1,4] diazepine group and simplified substituted phenyl to improve the inhibition for BRD4 (Figure 3). Thus, the novel 4,4-difluoro-1-methyl-*N*, 6-diphenyl-5, 6-dihydro-4*H*-pyrimido [4, 5-*b*] [1, 2, 4] triazolo [4, 3-*d*] [1, 4] diazepin-8-amine derivatives were designed based on the SARs of BI-2536.

2 | EXPERIMENTAL SECTION

2.1 | General chemistry experimental details

All materials, solvents, and reagents were obtained from commercial sources. Purifications were implemented by column chromatography in 200–300 mesh silica gel and monitored by thin-layer chromatography which was performed on GF/UV 254 plates and visualized by using UV light at 254/365 nm. The purity of the compounds was evaluated by HPLC (>95%). Liquid chromatography-mass spectrometer spectra (LC-MS) was carried out on Waters ACQUITY UPLC-TQD at 25°C in ESI mode. ^{1}H NMR spectrum and ^{13}C NMR spectrum were noted on Bruker AV300 (300 MHz). The unit of coupling constant (*J* value) is Hz. Chemical shifts were expressed in ppm (d) relative to tetramethyl silane (TMS) as internal standard.

2.1.1 | General procedure for the synthesis of compounds 15a ~ 16h

To a solution of benzotriazole (11.90 g, 99.89 mmol) and aniline **1** (8.61 ml, 99.89 mmol) in anhydrous ether (100 ml), 37% aqueous formaldehyde was added dropwise (7.95 ml, 99.89 mmol). Then the reaction mixture was stirred at room temperature for 6 hr. After the reaction was completed, the mixture was filtered. Then the filtration cake was washed with cold ether and dried to give **3** as loose white solid (12.5 g, yield: 56%).

To a solution of trimethylchlorosilane (4.64 ml, 53.52 mmol) and 300 mesh zinc powder (4.72 g, 71.36 mmol) under nitrogen in anhydrous THF (80 ml), ethyl difluoro bromoacetate (6.96 ml, 53.52 mmol) and compound **3** (8.0 g, 35.68 mmol) were added, respectively, below 0°C. Then the reaction mixture was stirred below 0°C for 3 hr. When the reaction was completed, saturated sodium bicarbonate solution (60 ml) was slowly added to the mixture. Then the mixture was stirred for 10 min at room temperature and filtered with diatomite. The filtrate was extracted with ether (60 ml × 3). The combined organic layers were washed with saturated saline, dried over anhydrous sodium sulfate, concentrated under reduced pressure, and purified by silica gel column chromatography to give **5** as colorless oil (6.7 g, yield: 82%).

To a solution of 2,4-dichloro-5-nitropyrimidine (7.82 g, 40.31 mmol) and anhydrous sodium bicarbonate (12.31 g, 0.15 mol) under nitrogen in anhydrous ethyl acetate (100 ml), compound **5** (8.4 g, 36.64 mmol) was added

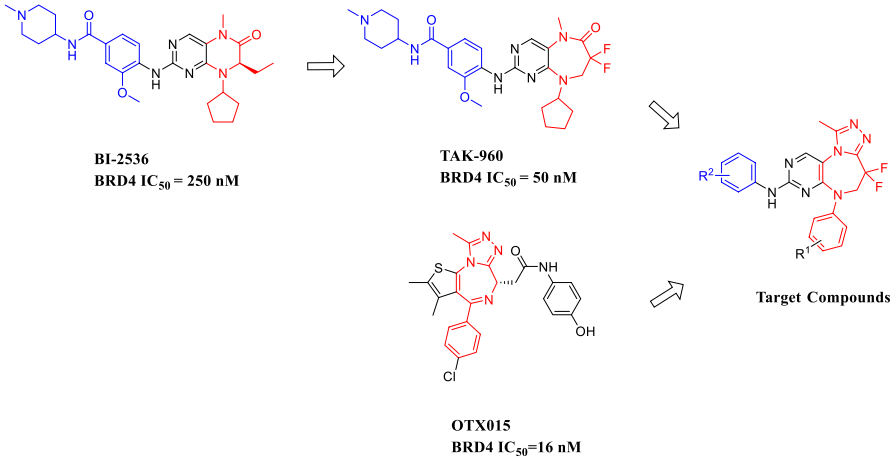

FIGURE 3 The design of the target compounds [Colour figure can be viewed at wileyonlinelibrary.com]

below 0°C. Then the mixture was stirred at room temperature for 16 hr. When the reaction was completed, the mixture was filtered with diatomite. Then the filtrate was washed with saturated saline (60 ml), dried over anhydrous sodium sulfate, concentrated under reduced pressure, and purified by silica gel column chromatography to give **7** as yellow solid (7.8 g, yield: 55%).

To a solution of compound **7** (6.5 g, 16.81 mmol) under nitrogen in acetic acid (50 ml), reduction iron powder (1.41 g, 25.21 mmol) was added. The mixture was stirred at 70°C for 1 hr and then at 100°C for 5 hr. When the reaction was completed, the mixture was filtered with diatomite. The filtrate was washed with saturated saline (40 ml), dried over anhydrous sodium sulfate, concentrated under reduced pressure, and purified by silica gel column chromatography to give **9** as yellow solid (3.2 g, yield: 61%).

To a solution of compound **9** (3.8 g, 12.23 mmol) in anhydrous tetrahydrofuran (50 ml), Lawesson reagent (2.97 g, 7.34 mmol) was added. The mixture was stirred at 70°C for 6 hr. When the reaction was completed, the mixture was diluted with water (20 ml) and extracted with dichloromethane (40 ml × 3). The combined organic layers were washed with saturated saline (40 ml), dried over anhydrous sodium sulfate, concentrated under reduced pressure, and purified by silica gel column chromatography to give **11** as yellow solid (2.6 g, yield: 65%).

To a solution of compound **11** (3.4 g, 10.41 mmol) in methanol and tetrahydrofuran (50 ml, V: V = 1:1), 80% hydrazine hydrate (6.51 ml, 0.10 mol) was added. The mixture was stirred at room temperature for 3 hr, and washed with saturated saline (40 ml × 2), dried over anhydrous sodium sulfate, and concentrated under reduced pressure to obtain intermediate when the reaction was completed. Then, triethyl orthoacetate (7.67 ml, 41.62 mmol) was added to a solution of intermediate in toluene (12 ml). Then the mixture was stirred at 110°C for 6 hr. When the reaction was completed, the mixture was diluted with water (6 ml) and extracted with ethyl acetate (20 ml × 3). The combined organic layers were washed with saturated saline, dried over anhydrous sodium sulfate, and purified by silica gel column chromatography to give **13** as white solid (2.6 g, yield: 72%).

To a solution of compound **13** (0.2 g, 0.57 mmol), aniline (0.059 g, 0.63 mmol) and cesium carbonate (0.37 g, 1.15 mmol) under nitrogen in 1,4-dioxane (40 ml), Tris (dibenzylacetone) diphenyl (52.52 mg, 0.057 mmol) and 4,5-bis (diphenylphosphine)—9,9-dimethoxyxanthene (0.37 g, 0.63 mmol) were added, respectively. Then the mixture was stirred at 110°C for 14 hr. When the reaction was completed, the mixture was diluted with water (20 ml) and extracted with ethyl acetate (50 ml × 3). The combined organic layers were washed with saturated saline (100 ml), dried over anhydrous sodium sulfate, and purified by silica gel column chromatography to afford target product **15a** as white solid (0.15 g, yield: 65%).

General procedure for the target compounds **15b~16h** was similar to that for compound **15a**.

*4,4-difluoro-1-methyl-*N*,6-diphenyl-5,6-dihydro-4*H*-pyrimido[4,5-*b*] [1,2,4] triazolo[4,3-*d*] [1,4] diazepin-8-amine (***15a***)*

White solid, yield 65%. m.p.: 156–158°C; ^{1}H NMR (300 MHz, DMSO-d_6) δ 9.71 (s, 1H), 8.63 (s, 1H), 7.48 (d, J = 7.0 Hz, 2H), 7.37 (d, J = 7.7 Hz, 3H), 7.19 (m, 2H), 6.95 (m, 2H), 6.82 (d, J = 6.7 Hz, 1H), 4.59 (t, J = 12.5 Hz, 2H), 2.63 (s, 3H). ^{13}C NMR (75 MHz, DMSO-d_6) δ 157.03, 153.67, 152.60, 145.32, 139.76, 129.45, 128.04, 125.88, 121.31, 118.24, 113.54, 58.01, 57.61, 57.20, 28.97, 11.90; LC-MS (ESI) *m/z*: 406.70 [M + H]$^+$; Anal. calcd. for $C_{21}H_{18}F_2N_7$: C, 62.22; H, 4.23; N, 24.18. Found: C, 62.24; H, 4.25; N, 24.22.

*4,4-difluoro-*N*-(4-methoxyphenyl)-1-methyl-6-phenyl-5,6-dihydro-4*H*-pyrimido[4,5-*b*] [1,2,4] triazolo[4,3-*d*] [1,4] diazepin-8-amine (***15b***)*

White solid, yield 68%. m.p.: 177–179°C; ^{1}H NMR (300 MHz, DMSO-d_6) δ 9.56 (s, 1H), 8.59 (s, 1H), 7.32 (m, 7H), 6.54 (s, 2H), 4.58 (t, J = 12.4 Hz, 2H), 3.65 (s, 3H), 2.62 (s, 3H). ^{13}C NMR (75 MHz, DMSO-d_6) δ 157.64, 153.63, 152.69, 145.31, 138.84, 129.62, 127.76, 126.18, 124.76, 119.59, 57.63, 31.10, 11.81; LC-MS (ESI) *m/z*: 436.07 [M + H]$^+$; Anal. calcd. for $C_{22}H_{20}F_2N_7O$: C, 60.68; H, 4.40; N, 22.52. Found: C, 60.62; H, 4.42; N, 22.54.

*N-(4-chlorophenyl)-4,4-difluoro-1-methyl-6-phenyl-5,6-dihydro-4*H*-pyrimido[4,5-*b*] [1,2,4]-triazolo[4,3-*d*] [1,4] diazepin-8-amine (***15c***)*

White solid, yield 65%. m.p.: 175–177°C; ^{1}H NMR (300 MHz, DMSO-d_6) δ 9.42 (s, 1H), 8.57 (s, 1H), 7.35 (m, 7H), 6.54 (s, 2H), 4.50 (t, J = 12.4 Hz, 2H), 3.64 (s, 3H), 2.66 (s, 3H). ^{13}C NMR (75 MHz, DMSO-d_6) δ 156.69, 153.69, 152.68, 145.31, 138.81, 129.62, 127.77, 126.18, 124.74, 119.59, 57.67, 31.10, 11.88. LC-MS (ESI) *m/z*: 440.30 [M + H]$^+$; Anal. calcd. for $C_{21}H_{17}ClF_2N_7$: C, 57.34; H, 3.67; N, 22.29. Found: C, 57.40; H, 3.62; N, 22.24.

*4,4-difluoro-*N*-(4-fluorophenyl)-1-methyl-6-phenyl-5,6-dihydro-4*H*-pyrimido[4,5-*b*] [1,2,4] triazolo[4,3-*d*] [1,4] diazepin-8-amine (***15d***)*

Brown solid, yield 62%. m.p.: 164–166°C; ^{1}H NMR (300 MHz, DMSO-d_6) δ 9.58 (s, 1H), 8.92 (s, 1H), 7.42 (m, 7H), 6.38 (s, 2H), 4.55 (t, J = 12.4 Hz, 2H), 3.60 (s, 3H), 2.64 (s, 3H). ^{13}C NMR (75 MHz, DMSO-d_6) δ 169.98, 167.32, 166.34, 161.02, 141.09, 138.68, 136.22, 131.15, 130.30, 130.24, 129.05, 124.41, 117.73, 116.48, 108.74, 95.93, 55.77, 45.87, 42.05, 34.43, 27.19, 25.86, 25.15, 23.87. LC-MS (ESI) *m/z*: 424.70 [M + H]$^+$; Anal. calcd.

for $C_{21}H_{17}F_3N_7$: C, 59.57; H, 3.81; N, 23.16. Found: C, 59.59; H, 3.82; N, 23.14.

N-*(3,4-dimethoxyphenyl)-4,4-difluoro-1-methyl-6-phenyl-5,6-dihydro-4*H-*pyrimido[4,5-*b*] [1,2,4] triazolo[4,3-*d*] [1,4] diazepin-8-amine (***15e***)*

White solid, yield 65%. m.p.: 168–170°C; ^{1}H NMR (300 MHz, DMSO-d_6) δ 9.84 (s, 1H), 8.67 (s, 1H), 7.35 (m, 6H), 6.52 (s, 2H), 4.52 (t, J = 12.4 Hz, 2H), 3.67 (s, 3H), 3.62 (s, 3H), 2.64 (s, 3H). ^{13}C NMR (75 MHz, DMSO-d_6) δ 157.43, 153.79, 152.52, 148.41, 145.04, 143.86, 133.36, 129.22, 124.95, 124.19, 111.91, 104.31, 78.43, 55.78, 55.21, 32.87, 31.24, 31.10, 31.04, 28.95, 11.81. LC-MS (ESI) *m/z*: 466.19 [M + H]$^+$; Anal. calcd. for $C_{23}H_{22}F_2N_7O_2$: C, 59.35; H, 4.55; N, 21.06. Found: C, 59.37; H, 4.52; N, 21.04.

N-*(4-(tert-butyl) phenyl)-4,4-difluoro-1-methyl-6-phenyl-5,6-dihydro-4*H-*pyrimido[4,5-*b*] [1,2,4] triazolo[4,3-*d*] [1,4] diazepin-8-amine (***15f***)*

Grayish white solid, yield 65%. m.p.: 145–147°C; ^{1}H NMR (300 MHz, DMSO-d_6) δ 9.61 (s, 1H), 8.61 (s, 1H), 7.23 (dd, J = 112.6, 37.2 Hz, 8H), 4.71–4.31 (m, 2H), 2.56 (d, J = 36.3 Hz, 3H), 1.20 (s, 9H). ^{13}C NMR (75 MHz, DMSO-d_6) δ 157.19, 153.67, 152.55, 145.33, 137.08, 129.41, 125.57, 124.57, 118.34, 31.16, 11.89. LC-MS (ESI) *m/z*: 462.19 [M + H]$^+$; Anal. calcd. for $C_{25}H_{26}F_2N_7$: C, 65.06; H, 5.46; N, 21.24. Found: C, 65.07; H, 5.42; N, 21.27.

N-*(2-chlorophenyl)-4,4-difluoro-1-methyl-6-phenyl-5,6-dihydro-4*H-*pyrimido[4,5-*b*] [1,2,4] triazolo[4,3-*d*] [1,4] diazepin-8-amine (***15g***)*

White solid, yield 65%. m.p.: 173–175°C; ^{1}H NMR (300 MHz, DMSO-d_6) δ 8.63 (d, J = 4.2 Hz, 2H), 7.55–7.21 (m, 7H), 6.94 (m, 2H), 4.59 (t, J = 12.4 Hz, 2H), 2.63 (s, 3H). ^{13}C NMR (75 MHz, DMSO-d_6) δ 170.14, 167.11, 161.04, 140.97, 138.78, 138.70, 136.24, 131.09, 130.91, 130.28, 129.08, 128.64, 124.49, 123.22, 118.91, 117.16, 116.55, 108.80, 95.83, 55.75, 37.75, 27.22. LC-MS (ESI) *m/z*: 440.30 [M + H]$^+$; Anal. calcd. for $C_{21}H_{17}ClF_2N_7$: C, 57.34; H, 3.67; N, 22.28. Found: C, 57.36; H, 3.62; N, 22.27.

*4,4-difluoro-1-methyl-*N-*(4-nitrophenyl)-6-phenyl-5,6-dihydro-4*H-*pyrimido[4,5-*b*] [1,2,4]-triazolo[4,3-*d*] [1,4] diazepin-8-amine (***15*h***)*

Yellow solid, yield 70%. m.p.: 166–168°C; ^{1}H NMR (300 MHz, DMSO-d_6) δ 10.45 (s, 1H), 8.69 (s, 1H), 8.00–6.93 (m, 8H), 4.61 (t, J = 12.4 Hz, 2H), 2.63 (s, 3H). ^{13}C NMR (75 MHz, DMSO-d_6) δ 170.16, 167.10, 167.03, 161.04, 156.31, 140.97, 138.70, 136.27, 135.16, 131.09, 131.02, 130.26, 130.20, 129.06, 124.46, 120.73, 120.62, 117.07, 116.51, 115.34, 115.27, 115.04, 108.82, 95.84, 55.74, 37.65, 27.19. LC-MS (ESI) *m/z*: 451.30 [M + H]$^+$; Anal. calcd. for $C_{21}H_{17}ClF_2N_8O_2$: C, 56.01; H, 3.58; N, 24.88. Found: C, 56.06; H, 3.56; N, 24.87.

*6-(4-chlorophenyl)-4,4-difluoro-1-methyl-*N-*phenyl-5,6-dihydro-4*H-*pyrimido[4,5-*b*] [1,2,4] triazolo[4,3-*d*] [1,4] diazepin-8-amine (***16a***)*

White solid, yield 61%. m.p.: 163–165°C; ^{1}H NMR (300 MHz, DMSO-d_6) δ 9.64 (s, 1H), 8.65 (s, 1H), 7.54 (d, J = 7.0 Hz, 2H), 7.28 (d, J = 7.7 Hz, 2H), 7.16 (m, 2H), 6.93 (m, 2H), 6.83 (d, J = 6.7 Hz, 1H), 4.58 (t, J = 12.5 Hz, 2H), 2.64 (s, 3H). ^{13}C NMR (75 MHz, DMSO-d_6) δ 168.59, 168.52, 167.74, 163.53, 159.01, 149.67, 148.71, 149.76, 145.76, 145.63, 145.01, 144.36, 144.31, 143.95, 140.25, 129.47, 129.19, 128.4, 128.28 128.12, 128.07, 124.73, 122.55, 122.51, 121.13, 119.81, 117.47, 54.87, 54.35, 53.90, 11.94. LC-MS (ESI) *m/z*: 440.02 [M + H]$^+$; Anal. calcd. for $C_{21}H_{17}ClF_2N_7$: C, 57.34; H, 3.67; N, 22.28. Found: C, 57.36; H, 3.65; N, 22.25.

*6-(4-chlorophenyl)-4,4-difluoro-*N-*(4-methoxyphenyl)-1-methyl-5,6-dihydro-4*H-*pyrimido-[4,5-*b*] [1,2,4] triazolo[4,3-*d*] [1,4] diazepin-8-amine (***16b***)*

White solid, yield 68%. m.p.: 169–171°C; ^{1}H NMR (300 MHz, DMSO-d_6) δ 9.59 (s, 1H), 8.59 (s, 1H), 7.47 (d, J = 46.9 Hz, 4H), 7.09 (s, 2H), 6.58 (s, 2H), 4.57 (t, J = 12.4 Hz, 2H), 3.67 (s, 3H), 2.61 (s, 3H). ^{13}C NMR (75 MHz, DMSO-d_6) δ 154.59, 154.29, 153.12, 147.90, 144.74, 133.33, 129.84, 113.62, 55.45, 12.34. LC-MS (ESI) *m/z*: 470.30 [M + H]$^+$; Anal. calcd. for $C_{22}H_{19}ClF_2N_7O$: C, 56.24; H, 3.86; N, 20.87. Found: C, 56.26; H, 3.82; N, 20.85.

N,*6-bis(4-chlorophenyl)-4,4-difluoro-1-methyl-5,6-dihydro-4*H-*pyrimido[4,5-*b*] [1,2,4]-triazolo[4,3-*d*] [1,4] diazepin-8-amine (***16c***)*

White solid, yield 75%. m.p.:174–176°C; ^{1}H NMR (300 MHz, DMSO-d_6) δ 9.90 (s, 1H), 8.64 (s, 1H), 7.30 (dd, J = 111.4, 52.8 Hz, 8H), 4.60 (t, J = 11.7 Hz, 2H), 2.56 (s, 3H). ^{13}C NMR (75 MHz, DMSO-d_6) δ 157.21, 154.32, 153.22, 147.92, 144.66, 139.24, 129.98, 128.27, 125.47, 120.32, 58.00, 12.35. LC-MS (ESI) *m/z*: 474.20 [M + H]$^+$; Anal. calcd. for $C_{21}H_{16}Cl_2F_2N_7$: C, 53.18; H, 3.19; N, 20.67. Found: C, 53.16; H, 3.17; N, 20.70.

*6-(4-chlorophenyl)-4,4-difluoro-*N-*(4-fluorophenyl)-1-methyl-5,6-dihydro-4*H-*pyrimido[4,5-*b*] [1,2,4] triazolo[4,3-*d*] [1,4] diazepin-8-amine (***16d***)*

Brown solid, yield 66%. m.p.: 154–156°C; ^{1}H NMR (300 MHz, DMSO-d_6) δ 9.78 (s, 1H), 8.62 (s, 1H), 7.54 (d, J = 8.2 Hz, 2H), 7.39 (d, J = 8.4 Hz, 2H), 7.22 (s, 2H), 6.80 (s, 2H), 4.58 (t, J = 12.6 Hz, 2H), 2.61 (s, 3H). ^{13}C NMR (75 MHz, DMSO-d_6) δ 157.26, 154.30, 153.26, 147.92, 144.67, 139.24, 129.92, 128.27, 125.43, 120.34, 58.06, 12.34. LC-MS (ESI) *m/z*: 458.32 [M + H]$^+$; Anal. calcd. For

$C_{21}H_{16}ClF_3N_7$: C, 55.09; H, 3.30; N, 21.42. Found: C, 55.06; H, 3.27; N, 21.47.

*6-(4-chlorophenyl)-4,4-difluoro-1-methyl-*N*-(4-(trifluoromethoxy) phenyl)-5,6-dihydro-4*H*-pyrimido[4,5-*b*] [1,2,4] triazolo[4,3-*d*] [1,4] diazepin-8-amine (***16e***)*

Dark brown solid, yield 64%. m.p.: 158–160°C; ^{1}H NMR (300 MHz, DMSO-d_6) δ 9.93 (s, 1H), 8.64 (s, 1H), 7.65–7.49 (m, 2H), 7.41 (d, J = 6.8 Hz, 2H), 7.36–7.17 (m, 2H), 7.03–6.82 (m, 2H), 4.59 (t, J = 11.4 Hz, 2H), 2.62 (s, 3H). ^{13}C NMR (75 MHz, DMSO-d_6) δ 157.21, 154.36, 153.20, 147.92, 144.68, 142.73, 139.51, 129.97, 121.88, 121.18, 119.99, 57.99, 12.38. LC-MS (ESI) m/z: 524.32 $[M + H]^+$; Anal. calcd. For $C_{22}H_{16}ClF_5N_7O$: C, 50.44; H, 2.89; N, 18.72. Found: C, 50.46; H, 2.85; N, 18.77.

N*-(4-(tert-butyl) phenyl)-6-(4-chlorophenyl)-4,4-difluoro-1-methyl-5,6-dihydro-4*H*-pyrimido-[4,5-*b*] [1,2,4] triazolo[4,3-*d*] [1,4] diazepin-8-amine (***16f***)*

Grayish white solid, yield 65%. m.p.: 162–164°C; ^{1}H NMR (300 MHz, DMSO-d_6) δ 9.63 (s, 1H), 8.58 (s, 1H), 7.58–7.32 (m, 4H), 7.15–6.89 (m, 4H), 4.57 (t, J = 11.4 Hz, 2H), 2.61 (s, 3H), 1.22 (s, 9H). ^{13}C NMR (75 MHz, DMSO-d_6) δ 157.00, 153.73, 152.63, 144.29, 143.81, 136.99, 129.41, 124.53, 118.30, 54.83, 33.69, 31.14, 30.64, 11.85. LC-MS (ESI) m/z: 496.24 $[M + H]^+$; Anal. calcd. For $C_{25}H_{25}ClF_2N_7$: C, 60.54; H, 4.88; N, 19.77. Found: C, 60.56; H, 4.85; N, 19.79.

N*-(3-chlorophenyl)-6-(4-chlorophenyl)-4,4-difluoro-1-methyl-5,6-dihydro-4*H*-pyrimido[4,5-*b*] [1,2,4] triazolo[4,3-*d*] [1,4] diazepin-8-amine (***16g***)*

White solid, yield 69%. m.p.: 166–168°C; ^{1}H NMR (300 MHz, DMSO-d_6) δ 8.67 (d, J = 4.2 Hz, 2H), 7.58–7.25 (m, 6H), 6.94 (m, 2H), 4.58 (t, J = 12.4 Hz, 2H), 2.64 (s, 3H). ^{13}C NMR (75 MHz, DMSO-d_6) δ 157.07, 156.84, 153.90, 152.66, 143.78, 141.20, 132.95, 130.20, 129.57, 129.37, 126.77, 121.24, 117.49, 116.75, 57.73, 57.32, 56.89, 11.86. LC-MS (ESI) m/z: 474.20 $[M + H]^+$; Anal. calcd. For $C_{21}H_{16}Cl_2F_2N_7$: C, 53.18; H, 3.19; N, 20.67. Found: C, 53.16; H, 3.21; N, 20.63.

*6-(4-chlorophenyl)-4,4-difluoro-1-methyl-*N*-(4-nitrophenyl)-5,6-dihydro-4*H*-pyrimido[4,5-*b*] [1,2,4] triazolo[4,3-*d*] [1,4] diazepin-8-amine (***16h***)*

White solid, yield 74%. m.p.: 178–180°C; ^{1}H NMR (300 MHz, DMSO-d_6) δ 10.48 (s, 1H), 8.71 (s, 1H), 7.87 (d, J = 8.4 Hz, 2H), 7.62 (d, J = 7.7 Hz, 2H), 7.48–7.27 (m, 4H), 4.62 (t, J = 12.0 Hz, 2H), 2.63 (s, 3H). ^{13}C NMR (75 MHz, DMSO-d_6) δ 170.16, 167.10, 167.03, 161.04, 140.97, 138.70, 136.27, 135.16, 131.09, 131.02, 130.26, 130.20, 129.06, 124.46, 120.73, 120.62, 117.07, 116.51, 115.34, 115.27, 115.04, 108.82, 95.84, 55.74, 37.65, 27.19. LC-MS (ESI) m/z: 485.37 $[M + H]^+$; Anal. calcd. For $C_{21}H_{16}ClF_2N_8O_2$: C, 52.02; H, 3.12; N, 23.11. Found: C, 52.06; H, 3.14; N, 23.14.

2.2 | Biological assays

2.2.1 | BRD4 inhibition TR-FRET assay

BRD4-BD1 TR-FRET Assay Kit (Cayman, 600520) was used to perform the BRD4 inhibition assay. All assays were carried out in coning 384 well plates. First, 10 μl of europium chloride solution of BRD4-BD1 was added to the 384 well plate and the plant was incubated in the dark for 15 min at room temperature. Then, 5 μl of BRD4 ligand/APC receptor complex was added to each well and the plant was incubated in the dark at room temperature for 1 hr. After the incubation, the plate was read on the PerkinElmer multimode plate reader with TR-FRET technique under 340 nm excitation and 670 nm emission/620 nm emission. The absorbance between the negative control and the target compounds was used to calculate the BRD4 inhibition rate, and IC_{50} values were calculated from the BRD4 inhibition rate.

2.2.2 | Cell growth inhibition assay

MV4-11 cells were cultured in IMDM modified with 10% FBS and 1% penicillin-streptomycin in Thermo CO_2 incubators at 37°C. Cells were collected in logarithmic growth phase, and then 100 μl of cell suspension containing 1×10^4 cells was added to each well of 96 well plate. The plate was incubated in Thermo CO_2 incubators at 37°C for 12 hr. After incubation, 10 μl of compounds with different concentrations were added to each well. After cultured for 72 hr, 5 μl of CCK-8 was added to each well. The plate was read on PerkinElmer multimode plate reader at 450 nm and IC_{50} values were calculated by GraphPad Prism 7 software.

2.2.3 | Apoptosis and cell cycle analysis assay

MV4-11 cells were cultured in IMDM modified with 10% FBS and 1% penicillin-streptomycin in Thermo CO_2 incubators at 37°C. The effects of the target compounds on apoptosis and cell cycle were analyzed by flow cytometry. Annexin V-FITC Apoptosis Detection Kit (KeyGEN BioTECH, KGA107) and Cell Cycle Detection Kit (KeyGEN BioTECH, KGA512) were used for cell apoptosis and cell cycle assay, respectively. Cells were treated with the compound **15h** for 24 hr.

2.2.4 | Western blotting

MV4-11 cells were cultured in IMDM modified with 10% FBS and 1% penicillin-streptomycin in Thermo CO_2 incubators at 37°C. Cells were collected in logarithmic phase and treated with the compounds with different concentrations for another 4 hr. In order to determine the corresponding protein concentration for further, the cells were put in 1.5 ml centrifuge tube after cracking at 4°C. After that, 10% separation adhesive and 4% concentration adhesive were prepared, and SDS-polyacrylamide gel was placed in an electrophoresis tank for sample loading, electrophoresis, and protein transfer. Subsequently, the PVDF membrane was washed three times with TBST for 10 min each, immersed in the 5% fat-free milk TBST solution, and placed in a shaker at room temperature for 2 hr to block the non-specific protein binding sites. PVDF membrane was transferred with primary antibody diluent at 4°C overnight and washed three times with TBST for 10 min each after the reaction. The secondary antibody was added and incubated for 2 hr before development. The primary antibodies against c-Myc and β-actin were purchased from Cell Signaling Technology. BCA Protein Assay Kit was purchased from Beyotime.

2.2.5 | Molecular docking calculations

We used Schrödinger 2018 for molecular docking calculations. The crystal structure of BRD4 (PDB ID: **4BJX**) was available from PDB. Proteins were prepared by Protein Preparation Wizard for adding missing hydrogens, creating disulfide bonds, and so on. Compounds were prepared by LigPrep module to generate 3D structures. Receptor Grid Generation was used to identify the ligand and Schrödinger XP precision was used to perform the calculation (Bi et al., 2019). The final result was chosen based on the structure of the lowest XP score (−3.373).

3 | RESULTS AND DISCUSSION

3.1 | Synthesis of the target compounds

General procedure for preparation of the target compounds was showed in Scheme 1. Initially, 37% formaldehyde was added to a mixture of aniline (**1**) and benzotriazole in diethyl ether to prepare compound **3**, and then zinc powder was added to a mixture of compound **3**, trimethylchlorosilane, and ethyl difluoroethyl bromide in THF to prepare compound **5**. Subsequently, 2,4-dichloro-5-nitropyrimidine was added to a mixture of compound **5** in ethyl acetate to prepare compound **7**, and then reduction iron powder was added to a mixture of compound **7** in acetic acid to prepare compound **9**. Lawesson Reagent was added to a mixture of compound **9** in tetrahydrofuran to prepare compound **11**, and then hydrazine hydrate and triethyl orthoacetate were added to a mixture of compound **11** in methanol and tetrahydrofuran to prepare the key intermediate **13**. Finally, the target products **15a~15h** were prepared from compound **13** and various substituents anilines. The synthesis of the target compounds **16a~16h** was similar to that of **15a~15h**.

Reagents and conditions: (i) benzotriazole, 37% HCHO, Et_2O, r.t, 6 hr; (ii) trimethylchlorosilane, zinc power (325 mesh), THF, ethyl bromodifluoroacetate, 10°C to r.t, 3–6 hr; (iii) 2,4-dichloro-5-nitropyrimidine, $NaHCO_3$, EtOAc, r.t, 16 hr; (iv) Fe, AcOH, 70°C, 1 hr, 100°C, 4–5 hr; (v) Lawesson Reagent, THF, reflux; (vi) hydrazine hydrate, THF/MeOH (v: v = 1:1), triethyl orthoacetate/toluene (v: v = 2:3), 110°C, 6h; (vii) anilines, $Pd_2(dba)_3$, Cs_2CO_3, xantphos, 1,4-dioxane, 110°C.

3.2 | BRD4 inhibitory activity assay

The inhibitory activities of the target compounds against BRD4 were tested in vitro by using the time-resolved fluorescence resonance energy transfer (TR-FRET)

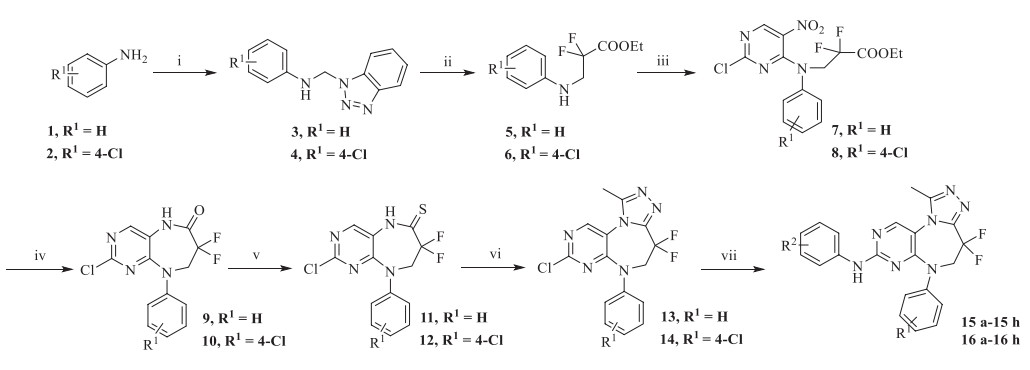

15 a: R^1=H, R^2=H
15 b: R^1=H, R^2=4-OCH_3
15 c: R^1=H, R^2=4-Cl
15 d: R^1=H, R^2=4-F
15 e: R^1=H, R^2=3,4-di-OCH_3
15 f: R^1=H, R^2=4-tertiary butyl
15 g: R^1=H, R^2=2-Cl
15 h: R^1=H, R^2=4-NO_2
16 a: R^1=4-Cl, R^2=H
16 b: R^1=4-Cl, R^2=4-OCH_3
16 c: R^1=4-Cl, R^2=4-Cl
16 d: R^1=4-Cl, R^2=4-F
16 e: R^1=4-Cl, R^2=4-OCF_3
16 f: R^1=4-Cl, R^2=4-tertiary butyl
16 g: R^1=4-Cl, R^2=3-Cl
16 h: R^1=4-Cl, R^2=4-NO_2

SCHEME 1 General procedure for preparation of the target compounds

binding assay. As shown in Table 1, the results exhibited that all that target compounds had good inhibition for BRD4-BD1, especially compound **15h** (IC_{50} value of 0.42 μM) and compound **16h** (IC_{50} value of 0.55 μM). Based on the results, the SARs were summarized that the inhibitory activity of the target compounds would be reduced when R^1 was substituted by chlorine, and the inhibitory activity would be increased significantly when R^2 was substituted by electron-withdrawing groups. In summary, when compared with BI-2536, the optimal compound **15h** demonstrated equivalent inhibitory activity against BRD4-BD1, which indicated that the 1-methy l-5,6-dihydro-4*H*-pyrimido[4,5-*b*] [1,2,4]-triazolo[4,3-*d*] [1,4] diazepin-8-amine skeleton could effectively simulate the structure of KAc.

TABLE 1 Structure and inhibitory activity of the target compounds (**15a~16h**) against BRD4-BD1

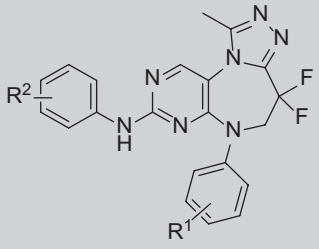

Compounds	R^1	R^2	IC_{50} (μM)[a]
15a	H	H	1.22 ± 0.01**
15b	H	4-OCH_3	0.86 ± 0.03*
15c	H	4-Cl	1.35 ± 0.04***
15d	H	4-F	0.94 ± 0.07*
15e	H	3,4-di-OCH_3	0.62 ± 0.01
15f	H	4-tertiary butyl	2.66 ± 0.11***
15g	H	2-Cl	0.68 ± 0.02*
15h	H	4-NO_2	0.42 ± 0.01
16a	4-Cl	H	1.62 ± 0.10***
16b	4-Cl	4-OCH_3	1.31 ± 0.08**
16c	4-Cl	4-Cl	2.63 ± 0.01***
16d	4-Cl	4-F	1.06 ± 0.04**
16e	4-Cl	4-OCF_3	1.54 ± 0.02***
16f	4-Cl	4-tertiary butyl	4.51 ± 0.02***
16g	4-Cl	3-Cl	1.32 ± 0.13***
16h	4-Cl	4-NO_2	0.55 ± 0.01
(+)-JQ−1	—	—	0.074 ± 0.003***
BI−2536	—	—	0.53 ± 0.04

[a]The IC_{50} value in the table was calculated from the TR-FRET assay. The data were expressed as the means ± *SD* ($n = 3$).

*$p < .05$, **$p < .01$, ***$p < .001$ versus compound **15h**.

3.3 | Cell growth inhibition assay

Using (+)-JQ-1 and BI-2536 as positive controls, we tested the anti-proliferative effects of the target compounds on MV4-11 (biphenotypic B myelomonocytic leukemia) cell lines. The results demonstrated that all the target compounds had inhibitory effects on MV4-11 (Table 2). Among these compounds, compound **15h** had outstanding inhibitory effect on MV4-11 cells (IC_{50} value of 0.51 μM), which was consistent with the results of the BRD4 inhibitory activity assay.

3.4 | Cell apoptosis, cell cycle analysis, and Western blotting assay

Flow cytometry was used to analyze the effect of compound **15h** on inducing apoptosis and cell cycle arrest in MV4-11 cell lines. As showed in Figure 4, compound **15h** had equivalent apoptosis-inducing effect on MV4-11 in a dose-dependent manner when compared with (+)-JQ-1 and compound **15h** and (+)-JQ-1 could arrest MV4-11 cells at G0/G1 phase in a dose-dependent manner significantly (Figure 5). It was reported that BRD4 worked as regulatory factors for c-Myc protein (Delmore et al., 2011). We performed the western blotting analysis to research the effects on c-Myc. Compound **15h** and (+)-JQ-1 were chosen to evaluate their effects on the expression of c-Myc. As shown in Figure 6, it was encouraging that compound **15h** downregulated the expression of c-Myc in a dose-dependent manner apparently. To sum up, the compound **15h** targeting BRD4 showed excellent inhibitory activities on protein and MV4-11 cell lines in vitro. And it could be further optimized and modified on the basis of the structure-activity relationships to obtain BRD4 inhibitors with higher safety and higher selectivity.

TABLE 2 The anti-proliferative effects of the target compounds on MV4-11

Compounds	IC_{50} (μM)[a]	Compounds	IC_{50} (μM)[a]
15a	3.09 ± 0.12***	**16a**	4.46 ± 0.62***
15b	1.15 ± 0.11*	**16b**	3.42 ± 0.25***
15c	3.56 ± 0.43***	**16c**	4.23 ± 0.46***
15d	2.74 ± 0.33**	**16d**	2.14 ± 0.73**
15e	0.76 ± 0.16	**16e**	3.79 ± 0.85***
15f	4.57 ± 0.84***	**16f**	8.85 ± 1.12***
15g	1.02 ± 0.46*	**16g**	3.57 ± 0.26***
15h	0.51 ± 0.17	**16h**	0.76 ± 0.22
(+)-JQ-1	0.16 ± 0.05*	BI-2536	0.68 ± 0.06

[a]The IC_{50} value in the table was calculated from the CCK-8 assay. The data were expressed as the means ± *SD* ($n = 3$).

*$p < .05$, **$p < .01$, ***$p < .001$ versus compound **15h**.

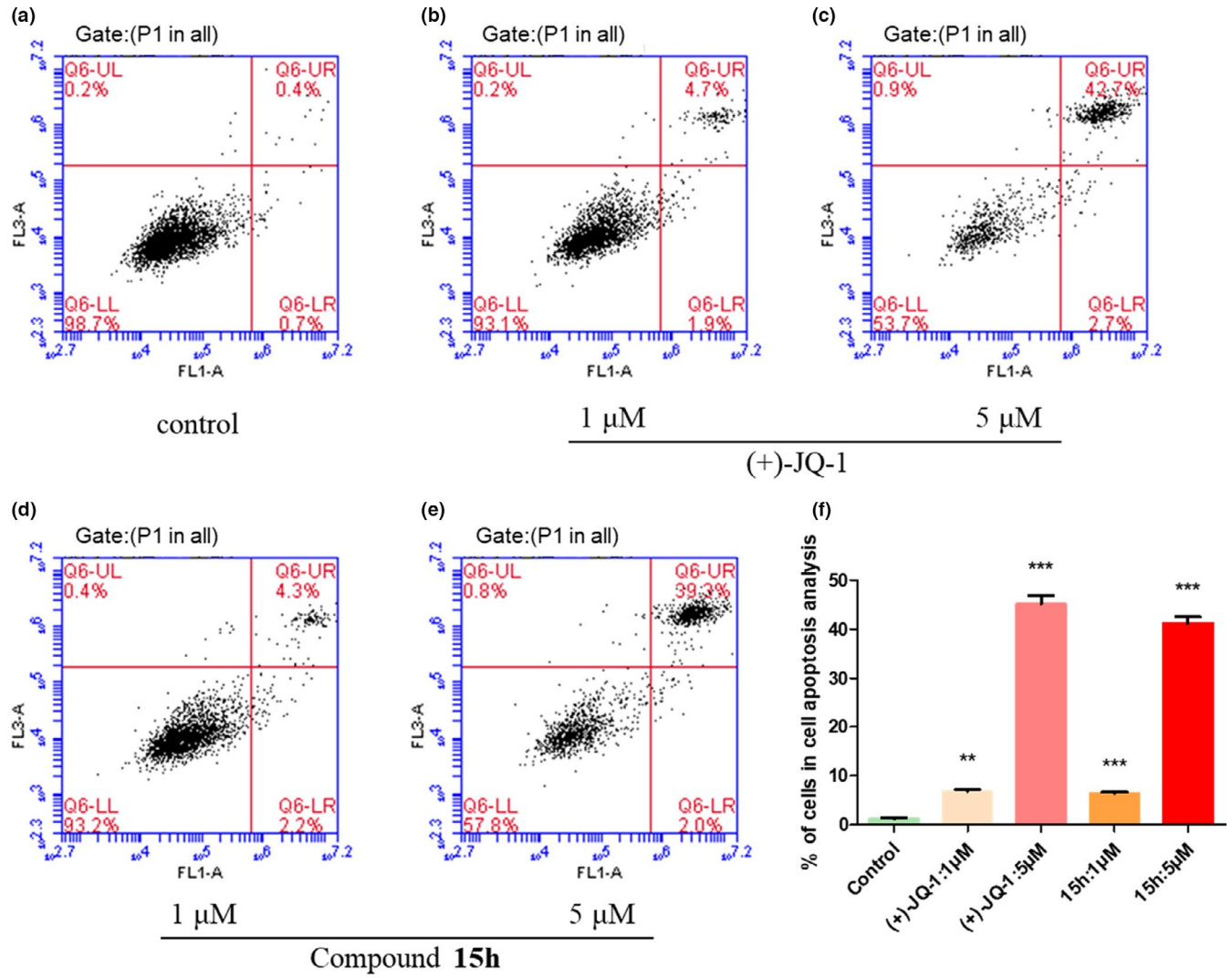

FIGURE 4 Effects of (+)-JQ-1 and compound **15h** on apoptosis in MV4-11 cells: (a) Control; (b) (+)-JQ-1(1 μM); (c) (+)-JQ-1 (5 μM); (d) Compound **15h** (1 μM); (e) Compound **15h** (5 μM); (f) Cell apoptosis analysis, the values were expressed as the means ± *SD* ($n = 3$). $^{**}p < .01$, $^{***}p < .001$ versus control group [Colour figure can be viewed at wileyonlinelibrary.com]

3.5 | Molecular docking study

Schrödinger was used to analyze the possible binding mode between compound **15h** and BRD4-BD1 (PDB ID: **4BJX**). As expected, compound **15h** (Figure 7a) and (+)-JQ-1 (Figure 2a) had the equivalent binding mode with BRD4-BD1, they could directly form key hydrogen bonds with Tyr 97 via a water molecule and Asn140 in BRD4-BD1. Moreover, the docking results showed that compound **15h** formed the pi–pi stacking with Trp81 in BRD4-BD1 and the molecular structure of compound **15h** had interaction with the WPF (Trp81, Pro82, Phe83) shelf of BRD4-BD1 (Figure 7b).

4 | CONCLUSION

In summary, we have taken BI-2536 as the lead compound to design and synthesize the target compounds with the core structure (**1-methyl-5,6-dihydro-4*H*-pyrimido[4,5-*b*] [1,2,4]-triazolo[4,3-*d*] [1,4] diazepin-8-amine**). The results of BRD4 inhibitory activity assay in vitro showed that the target compounds had good inhibitory activities against BRD4-BD1. Among the target compounds, compound **15h** showed excellent BRD4-BD1 inhibitory activity (IC_{50} value of 0.42 μM), which was equivalent to that of BI-2536 (IC_{50} value of 0.53 μM). Correspondingly, compound **15h** had outstanding inhibitory effect on MV4-11 cells in the cell growth inhibition assay (IC_{50} value of 0.51 μM). Furthermore, compound **15h** had potent apoptosis-inducing effect on MV4-11 cells and could arrest MV-4-11 cells at G0/G1 phase in a dose-dependent manner significantly. In Western blotting assay, compound **15h** down-regulated the expression of c-Myc apparently. Moreover, based on the docking results, compound **15h** could form key hydrogen bonds with

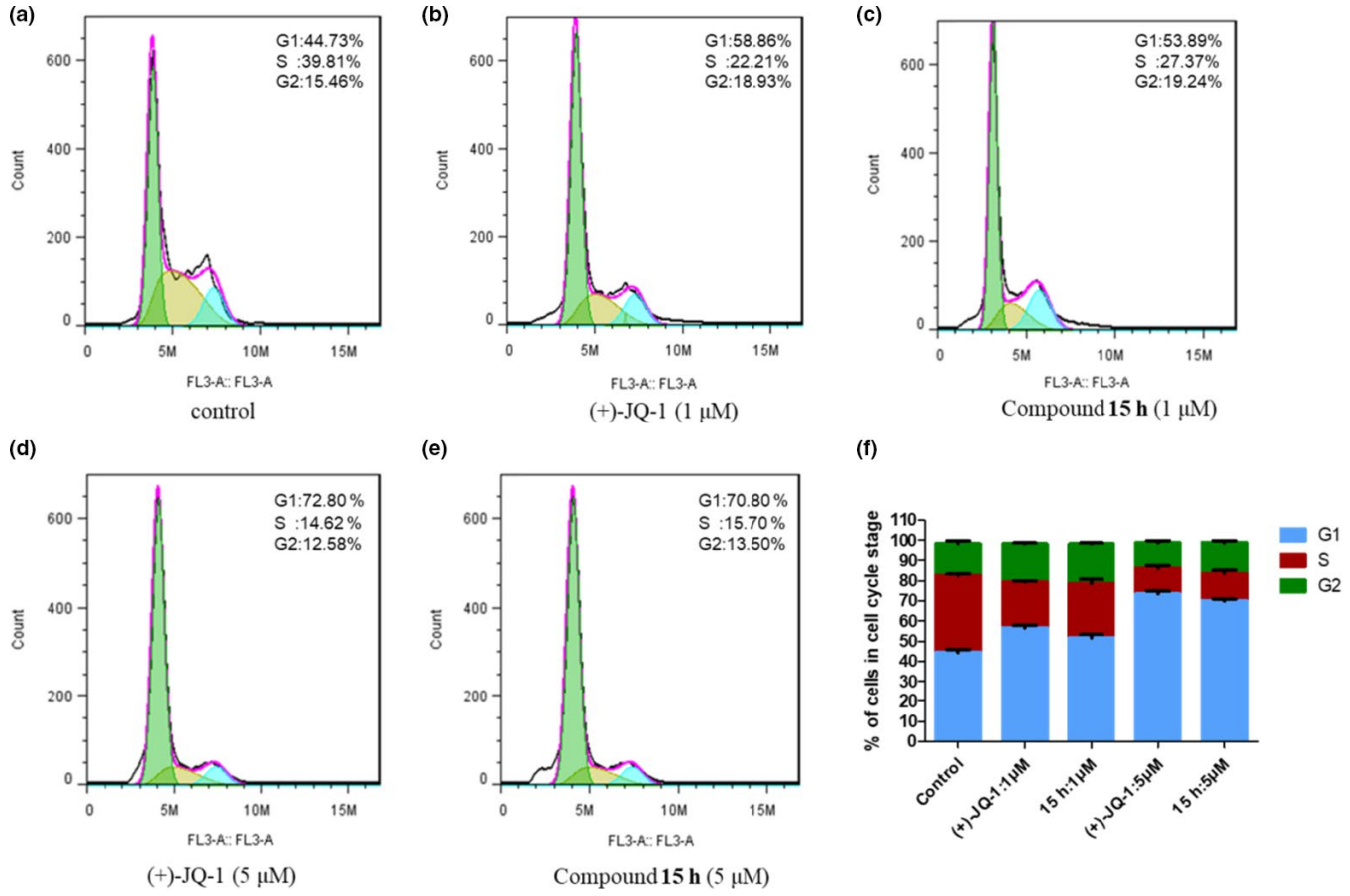

FIGURE 5 Effects of (+)-JQ-1 and compound **15h** on cell cycle arrest in MV4-11 cells: (a) Control; (b) (+)-JQ-1(1 μM); (c) Compound **15h** (1 μM); (d) (+)-JQ-1 (5 μM); (e) Compound **15h** (5 μM); (f) Cell cycle analysis, MV4-11 cells were induced to arrest at G0/G1 phase in a dose-dependent manner [Colour figure can be viewed at wileyonlinelibrary.com]

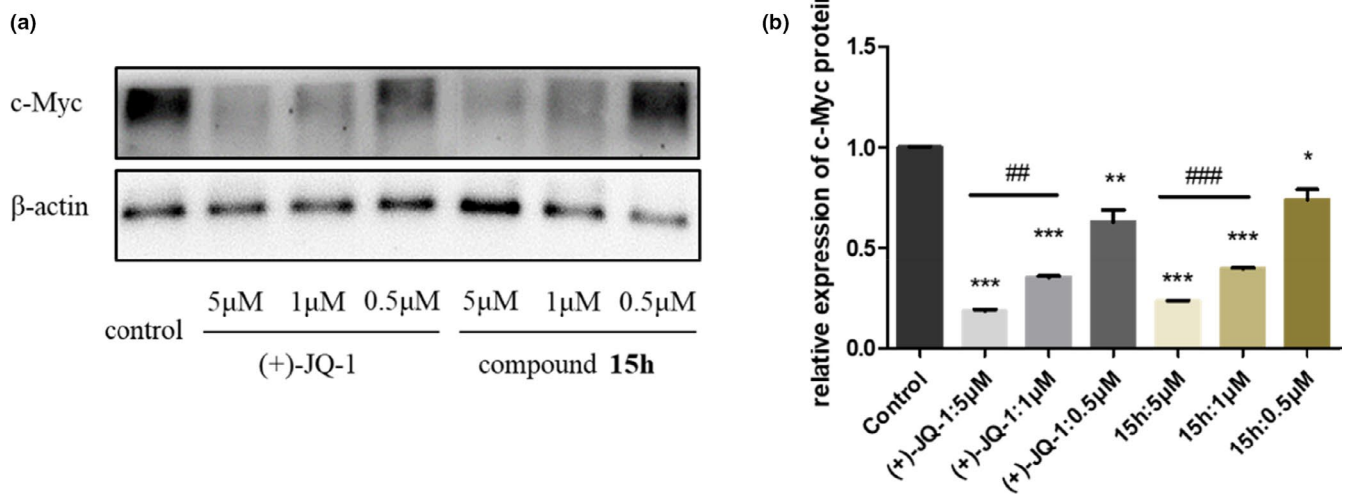

FIGURE 6 Effects of compound **15h** on the expression of c-Myc in MV4-11 cells: (a) Representative western blotting band of c-Myc in MV4-11 cells treated with (+)-JQ-1 and compound **15h**; (b) Band intensity of c-Myc expression analysis, the values were expressed as the means ± *SD* ($n = 3$). $^{*}p < .05$, $^{**}p < .01$, $^{***}p < .001$ versus control group, $^{\#\#}p < .01$, $^{\#\#\#}p < .001$ [Colour figure can be viewed at wileyonlinelibrary.com]

Tyr97 via a water molecule and Asn140 in BRD4-BD1 directly, which further indicated that the target compounds had better binding affinity to BRD4-BD1. Obviously, it can be confirmed that compound **15h** could be an effective BRD4 inhibitor and be utilized as an optimal compound for further development.

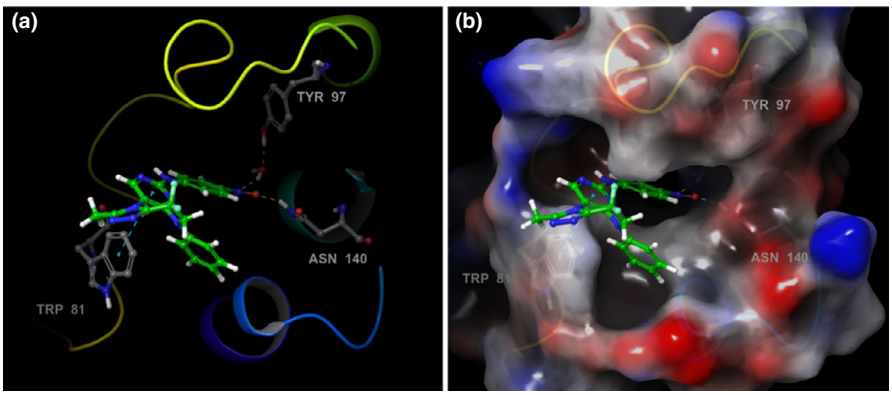

FIGURE 7 Docking results of compound **15h** with BRD4-BD1 (PDB ID: **4BJX**): (a) Compound **15h** could form hydrogen bonds with residue Tyr97 via a water molecule and Asn140, and form the pi-pi stacking with Trp81 in KAc recognition region of BRD4-BD1; (b) The binding site of compound **15h** in BRD4 [Colour figure can be viewed at wileyonlinelibrary.com]

ACKNOWLEDGMENTS

This study was supported by the National Science Foundation of China (No. 81872733) and the China Postdoctoral Science Foundation (No. 2020M681792).

CONFLICT OF INTEREST

All authors report no conflict of interest.

DATA AVAILABILITY STATEMENT

The data that supports the findings of this study are available in the supplementary material of this article.

ORCID

Hai Qian https://orcid.org/0000-0002-3827-0992

REFERENCES

Andrikopoulou, A., Liontos, M., Koutsoukos, K., Dimopoulos, M. A., & Zagouri, F. (2020). The emerging role of BET inhibitors in breast cancer. *Breast*, *53*, 152–163.

Bi, X., Li, J., Li, J., Shi, W., Dai, Y., Li, Q., Zhang, W., Huang, W., Qian, H., & Jiang, C. (2019). Design, synthesis and biological evaluation of novel 4,5-dihydro-[1,2,4]triazolo[4,3-f]pteridine derivatives as potential BRD4 inhibitors. *Bioorganic & Medicinal Chemistry*, *27*(13), 2813–2821.

Chen, L., Yap, J. L., Yoshioka, M., Lanning, M. E., Fountain, R. N., Raje, M., Scheenstra, J. A., Strovel, J. W., & Fletcher, S. (2015). BRD4 structure-activity relationships of dual PLK1 kinase/BRD4 bromodomain inhibitor BI-2536. *ACS Medicinal Chemistry Letters*, *6*(7), 764–769.

Chen, P., Yang, Y. F., Yang, L. Y., Tian, J. P., Zhang, F. Q., Zhou, J. P., & Zhang, H. B. (2019). 3-Hydroxyisoindolin-1-one derivates: Synthesis by palladium-catalyzed C-H activation as BRD4 inhibitors against human acute myeloid leukemia (AML) cells. *Bioorganic Chemistry*, *86*, 119–125.

Ciceri, P., Muller, S., O'Mahony, A., Fedorov, O., Filippakopoulos, P., Hunt, J. P., Lasater, E. A., Pallares, G., Picaud, S., Wells, C., Martin, S., Wodicka, L. M., Shah, N. P., Treiber, D. K., & Knapp, S. (2014). Dual kinase-bromodomain inhibitors for rationally designed polypharmacology (vol 10, pg 305, 2014). *Nature Chemical Biology*, *10*(8), 692.

Delmore, J. E., Issa, G. C., Lemieux, M. E., Rahl, P. B., Shi, J. W., Jacobs, H. M., Kastritis, E., Gilpatrick, T., Paranal, R. M., Qi, J., Chesi, M., Schinzel, A. C., McKeown, M. R., Heffernan, T. P., Vakoc, C. R., Bergsagel, P. L., Ghobrial, I. M., Richardson, P. G., Young, R. A., … Mitsiades, C. S. (2011). BET bromodomain inhibition as a therapeutic strategy to target c-Myc. *Cell*, *146*(6), 903–916.

Duan, Y., Guan, Y., Qin, W., Zhai, X., Yu, B., & Liu, H. (2018). Targeting Brd4 for cancer therapy: Inhibitors and degraders. *Medchemcomm*, *9*(11), 1779–1802.

Filippakopoulos, P., Qi, J., Picaud, S., Shen, Y., Smith, W. B., Fedorov, O., Morse, E. M., Keates, T., Hickman, T. T., Felletar, I., Philpott, M., Munro, S., McKeown, M. R., Wang, Y. C., Christie, A. L., West, N., Cameron, M. J., Schwartz, B., Heightman, T. D., … Bradner, J. E. (2010). Selective inhibition of BET bromodomains. *Nature*, *468*(7327), 1067–1073.

Fu, L. L., Tian, M., Li, X., Li, J. J., Huang, J., Ouyang, L., Zhang, Y. H., & Liu, B. (2015). Inhibition of BET bromodomains as a therapeutic strategy for cancer drug discovery. *Oncotarget*, *6*(8), 5501–5516.

Huang, W., Zheng, X., Yang, Y., Wang, X., & Shen, Z. (2016). An overview on small molecule inhibitors of BRD4. *Mini Reviews in Medicinal Chemistry*, *16*(17), 1403–1414.

Jung, M., Gelato, K. A., Fernandez-Montalvan, A., Siegel, S., & Haendler, B. (2015). Targeting BET bromodomains for cancer treatment. *Epigenomics*, *7*(3), 487–501.

Kharenko, O. A., Patel, R. G., Brown, S. D., Calosing, C., White, A., Lakshminarasimhan, D., Suto, R. K., Duffy, B. C., Kitchen, D. B., McLure, K. G., Hansen, H. C., van der Horst, E. H., & Young, P. R. (2018). Design and characterization of novel covalent bromodomain and extra-terminal domain (BET) inhibitors targeting a methionine. *Journal of Medicinal Chemistry*, *61*(18), 8202–8211.

Leal, A. S., Williams, C. R., Royce, D. B., Pioli, P. A., Sporn, M. B., & Liby, K. T. (2017). Bromodomain inhibitors, JQ1 and I-BET 762, as potential therapies for pancreatic cancer. *Cancer Letters*, *394*, 76–87.

Liu, Z. X., Sun, Q. R., & Wang, X. S. (2017). PLK1, a potential target for cancer therapy. *Translational Oncology*, *10*(1), 22–32.

Ran, X., Zhao, Y., Liu, L., Bai, L., Yang, C. Y., Zhou, B., Meagher, J. L., Chinnaswamy, K., Stuckey, J. A., & Wang, S. (2015). Structure-based design of gamma-carboline analogues as potent and specific BET bromodomain inhibitors. *Journal of Medicinal Chemistry*, *58*(12), 4927–4939.

Stathis, A., Zucca, E., Bekradda, M., Gomez-Roca, C., Delord, J. P., Rouge, T. D., Uro-Coste, E., de Braud, F., Pelosi, G., & French, C. A. (2016). Clinical response of carcinomas harboring the BRD4-NUT oncoprotein to the targeted bromodomain inhibitor OTX015/MK-8628. *Cancer Discovery*, *6*(5), 492–500.

Steegmaier, M., Hoffmann, M., Baum, A., Lenart, P., Petronczki, M., Krssak, M., Gurtler, U., Garin-Chesa, P., Lieb, S., Quant, J., Grauert, M., Adolf, G. R., Kraut, N., Peters, J. M., & Rettig, W. J. (2007). BI 2536, a potent and selective inhibitor of polo-like kinase 1, inhibits tumor growth in vivo. *Current Biology*, *17*(4), 316–322.

Wang, J., Chen, J., Jin, H., Lin, D., Chen, Y., Chen, X., Wang, B., Hu, S., Wu, Y., Wu, Y., Zhou, Y., Tian, N., Gao, W., Wang, X., & Zhang, X. (2019). BRD4 inhibition attenuates inflammatory response in microglia and facilitates recovery after spinal cord injury in rats. *Journal of Cellular and Molecular Medicine*, *23*(5), 3214–3223.

White, M. E., Fenger, J. M., & Carson, W. E. III (2019). Emerging roles of and therapeutic strategies targeting BRD4 in cancer. *Cellular Immunology*, *337*, 48–53.

Yoshida, G. J. (2018). Emerging roles of Myc in stem cell biology and novel tumor therapies. *Journal of Experimental & Clinical Cancer Research*, *37*(1), 173.

Zhang, Z. F., Ma, P. F., Jing, Y., Yan, Y., Cai, M. C., Zhang, M. Y., Zhang, S. Z., Peng, H. X., Ji, Z. L., Di, W., Gu, Z. Y., Gao, W. Q., & Zhuang, G. L. (2016). BET bromodomain inhibition as a therapeutic strategy in ovarian cancer by downregulating FoxM1. *Theranostics*, *6*(2), 219–230.

Zhao, L. L., Cao, D. Y., Chen, T. T., Wang, Y. Q., Miao, Z. H., Xu, Y. C., Chen, W. Y., Wang, X., Li, Y. D., Du, Z. Y., Xiong, B., Li, J., Xu, C. Y., Zhang, N. X., He, J. H., & Shen, J. K. (2013). Fragment-based drug discovery of 2-thiazolidinones as inhibitors of the histone reader BRD4 bromodomain. *Journal of Medicinal Chemistry*, *56*(10), 3833–3851.

Zhou, Y., Gu, Y., & Liu, J. M. (2019). BRD4 suppression alleviates cerebral ischemia-induced brain injury by blocking glial activation via the inhibition of inflammatory response and pyroptosis. *Biochemical and Biophysical Research Communications*, *519*(3), 481–488.

How to cite this article: Li J, Zhang W, Qiu Q, et al. Design, synthesis, and biological evaluation of novel 4,4-difluoro-1-methyl-*N*, 6-diphenyl-5, 6-dihydro-4*H*-pyrimido [4, 5-*b*] [1, 2, 4] triazolo [4, 3-*d*] [1, 4] diazepin-8-amine derivatives as potential BRD4 inhibitors. *Chem Biol Drug Des*. 2021;97:1117–1128. https://doi.org/10.1111/cbdd.13833